Journal of Statistical Physics, Vol. 30, No. 2, 1983

Random Walk of Dislocations Following a High-Velocity Impact

Bruce J. West[1] and Michael F. Shlesinger[1,2]

The permanent distortion of an elastic material due to a shock wave generated by a high-velocity impact is modeled by a random walk of dislocations. The dislocation movement is inhibited by a spatial and energetic distribution of activation barriers. The dislocations also experience a radially outward stress bias from the point of impact. The experimentally observed scaling of the total integrated momentum as well as the scaling with time of the penetration distance and strength of the shock wave are obtained in this model.

KEY WORDS: Biased random walk; dislocations; scaling; irreversible deformation.

1. INTRODUCTION

Random walk models have been highly successful in describing charge transport in amorphous materials probed via time-of-flight experiments.[1,2] The transport is characterized by a charged current which decays algebraically in time, even though the sample is placed in a high electric field. Instead of having a well-defined transit time through the sample (usually of the order of milliseconds) a steadily decreasing current persists for minutes or longer. This unusual time dependence can be generated by a highly non-Gaussian stochastic process which represents a random walk in a random medium. Various scaling laws and a universal behavior arise from this model in agreement with experiments.

Presented at the Symposium on Random Walks, Gaithersburg, MD, June 1982.

Research supported by Defense Advanced Research Projects Agency.

[1] Center for Studies of Nonlinear Dynamics, La Jolla Institute, P.O. Box 1434, La Jolla, California 92038.

[2] Permanent address: Institute for Physical Science and Technology, University of Maryland, College Park, Maryland 20742.

0022-4715/83/0200-0527$03.00/0

We present a similar random walk model for the formation of a distortion of a material following a high-velocity impact. A permanent distortion will form in a matter of tens of microseconds. Even in this short time span the damage can be separated into an early stage (roughly coinciding with the formation of a crater) and a late stage plastic flow.[3] An important feature is that the late stage flow will grow with a velocity which decreases algebraically with time, thus allowing a mathematical analogy to the charge transport in amorphous materials. The growth of the distortion will be related to a conservation law which is neither that of energy nor momentum. In Section 2 we review the phenomena of damage due to high-velocity impacts, and we present and analyze a random walk model in Section 3. In Section 4 we compare our scaling results with experiments.

2. THE PHENOMENA

An example of a high-velocity impact is a small meteorite striking a satellite. Obviously, a theory of the damage incurred as a function of the mass, speed, and angle of incidence of the projectile would be welcome. Unfortunately, the physical mechanisms governing the generation and propagation of damage in elastic materials due to high-velocity impacts are not yet understood. However, a number of useful phenomenological relations have been found, despite the fact that the appropriate macroscopic or microscopic equations for irreversible damage are not known.[3]

It is experimentally well established that the high-velocity impact of a hard projectile on a hard target (e.g., steel on steel) can result in both materials undergoing severe distortion with melting sometimes occurring. A hemispherical crater is formed on the target surface for normal incidence scattering. In the formation of the crater, target material is ejected away from the target as well as being convected into the target to form a shock wave. The speed of the shock exceeds the sound speed of the material. With the passage of the shock the material adjusts itself into a permanently deformed configuration. When the shock is weakened enough to become an elastic wave the plastic flow of the material ceases.

Using macroscopic concepts, experimental data, and large-scale computer calculations one describes the crater depth, D, via

$$\frac{D}{L} = K\left(\frac{\rho_p}{\rho_t}\right)^{1/3}\left(\frac{v_0}{c_0}\right)^{\alpha} \tag{1}$$

where L^3 is proportional to the projectile mass M, ρ_p and ρ_t are the projectile and target mass densities, v_0 is the projectile's initial velocity, c_0 is the material's sound velocity, and K characterizes the strength of the target.

An $\alpha = 2/3$ would arise from energy conservation, i.e., if the crater volume was proportional to the initial kinetic energy of the projectile. The experimental value of α is approximately 0.58 for steel-on-steel collisions.

One does not expect momentum conservation ($\alpha = 1/3$) for just the target because material is thrown backward resulting in a final momentum deposition in the target that can be many times larger than the incident projectile momentum. The ratio r of target to projectile momentum is found to scale as

$$r = (\text{const})v_0^{3\alpha - 1} \tag{2}$$

Equations (1) and (2) will be shown to be consistent with the conservation law

$$Mv_0^{3\alpha} = \text{const} \tag{3}$$

This implies that as long as Eq. (3) is valid projectiles with different M and v_0 values will cause equal damage.

3. THE MODEL: RANDOM WALK OF DISLOCATIONS

3.1. Physical Concepts

The strategy we now employ is to examine a simple microscopic model of the elastic and plastic properties of metal targets to provide a theoretical underpinning for Eqs. (1)–(3). Metals are composed of grains approximately 0.025 cm in linear extent. Each grain is a single crystal, and a macroscopic piece of metal consists of an agglomeration of randomly oriented crystals joined along an irregular honeycomb of common boundaries. In addition to grain boundaries there are dislocations, disinclinations, and combinations of both, such as screw dislocations. Dislocations break translational symmetry and allow atomic planes to slip when subject to a sufficient stress. In metals the number of dislocations is of the order of 10^{12} m^{-2}, and this number can be increased to 10^{15}–10^{16} m^{-2} after strengthening by rolling, etc. We assume that the generation of dislocations is the dominant mechanism for absorbing the energy of the shock wave as it passes through the metal. The generated dislocations can migrate in the stress field set up by the shock. Due to the grainy nature of the metal and the existence of imperfections such as voids, inclusions, etc., a dislocation may be trapped in a random network of imperfections characterized by a random set of activation energies. Dislocation transport becomes a succession of slips from one trapping site to another. We model this in Section 3.2 by a random walk on a lattice with a waiting-time distribution governing the time between slippings.

Some related ideas using absolute rate theory[4] have been applied to viscoelastic flows by relating the speed of the dislocation to $\exp(-U/kT)$, where U is the activation energy to escape a trap and T is the temperature of the lattice.

3.2. Mathematical Concepts

While we apply a random walk model in a novel manner to analyze the formation of a distortion in a solid, all the mathematics of the model has been previously discussed.[1,2,5–8] The dislocation motion is governed by a master equation with random transition rates. Klafter and Silbey[7] have shown by averaging over all configurations that the master equation exactly becomes a generalized master equation on a perfect lattice, and Kenkre *et al.*[8] have shown this to be equivalent to the continuous-time random walk (CTRW) of Montroll and Weiss.[5]

In addition to the initial condition, two quantities completely describe the CTRW; they are as follows:

(i) $p(\mathbf{l})$ = Prob. (a single jump is of displacement $\mathbf{l}$).

(ii) $\psi(t)dt$ = Prob. [jump occurring in the interval $(t, t+dt)$ given that the previous jump occurred at time $t=0$].

The probability $P(\mathbf{l}, t)$ to be at site $\mathbf{l}$ at time t is most easily given in Fourier ($\mathbf{l} \to \mathbf{k}$) and Laplace ($t \to u$) space, i.e.,

$$\tilde{P}^*(\mathbf{k}, u) = \left[1 - \tilde{p}(\mathbf{k})\psi^*(u)\right]^{-1} u^{-1}\left[1 - \psi^*(u)\right] \tag{4}$$

where

$$\tilde{p}(\mathbf{k}) \equiv \sum \cdots_{\mathbf{l}} \sum \exp(i\mathbf{k} \cdot \mathbf{l}) p(\mathbf{l}) \tag{5}$$

and

$$\psi^*(u) \equiv \int_0^\infty \exp(-ut)\psi(t)\, dt \tag{6}$$

The mean position, say in the jth direction, as a function of time is given by[6]

$$\langle l_j(t)\rangle \equiv \sum \cdots_{\mathbf{l}} \sum l_j P(\mathbf{l}, t) = -i\bar{l}_j \mathscr{L}^{-1}\left[\frac{\psi^*(u)}{u(1-\psi^*(u))}\right] \tag{7}$$

where $\mathscr{L}^{-1}$ is the inverse Laplace transform, and $\bar{l}_j = -i\partial\tilde{p}(\mathbf{k})/\partial k_j|_{\mathbf{k}=0}$ is the mean single jump distance in the jth direction.

Several classes of behavior are possible for $\langle l_j(t)\rangle$ depending on whether the moments of $p(\mathbf{l})$ and $\psi(t)$ are finite or infinite. If $p(\mathbf{l})$ and $\psi(t)$ are made dependent on each other then even more types of behavior are possible. We will discuss two cases. First, if at least two moments of $p(\mathbf{l})$

and one of $\psi(t)$ are finite then Gaussian behavior results as $t \to \infty$, and

$$\langle l_j(t)\rangle \sim \bar{l}_j t \tag{8}$$

If, however, $\overline{l_j^2} < \infty$ (for all j), but $\psi(t) \sim t^{-1-\beta}$ as $t \to \infty$ with $0 < \beta < 1$, then

$$\bar{t} \equiv \int_0^\infty t\psi(t)\,dt = \infty \tag{9}$$

and

$$\langle l_j(t)\rangle \sim \bar{l}_j t^\beta \tag{10}$$

a sublinear growth. It is possible to construct $\psi(t)$'s so Eq. (10) would involve logarithmic terms or other slowly varying functions.

While the analysis leading to Eq. (10) was a key to understanding the non-Gaussian nature of transport in amorphous materials similar ideas were not unknown to mathematicians. In his book, Feller[9] briefly alludes (in small print) at the end of a section on renewal theory to the possibility of a sublinear growth in time of the number of renewals. However, Feller[9] also remarks on using what are essentially nonexponential $\psi(t)$'s by writing "The generality is somewhat deceptive because it is hard to find practical examples besides the bus running without a schedule along a circular route." Transport in amorphous materials, and damage in metals due to high-velocity impacts, are practical examples.

We now choose explicit forms for $p(\mathbf{l})$ and $\psi(t)$. In three dimensions set

$$\begin{gathered} p(0, \pm 1, 0) = p(0, 0, \pm 1) = m, \\ p(1,0,0) = 2fn, \qquad p(-1,0,0) = 2(1-f)n \end{gathered} \tag{11}$$

where $4m + 2n = 1$ for conservation of probability. This $p(\mathbf{l})$ describes a random walk with a bias for steps in the positive x direction when $2n > 4m$ and $f > 1/2$. The mean position $\langle l_x(t)\rangle$ will have the same temporal behavior as a spherical symmetric model with an outward radial bias. Our choice of $p(\mathbf{l})$ in Cartesian coordinates is somewhat easier to manipulate than those in spherical coordinates.

In an unstressed metal we would choose

$$\psi(t) = \lambda \exp(-\lambda t) \tag{12}$$

with

$$\lambda = \lambda_0 \exp(-\epsilon/kT) \tag{13}$$

where ϵ is a barrier height, T is the temperature of the lattice, and λ_0 a frequency prefactor. However, if the distortion of the metal, due to the shock propagation, forces the dislocations to experience a distribution $g(\epsilon)$ of barrier heights, then $\psi(t)$ will be described by a distribution of rates $\rho(\lambda)$, i.e.,

$$\psi(t) = \int_0^\infty \lambda \exp(-\lambda t)\rho(\lambda)\, d\lambda \tag{14}$$

If one chooses

$$g(\epsilon) = \begin{cases} g_0 \exp(-\epsilon/kT_0) & \text{if} \quad \epsilon_0 \leqslant \epsilon \leqslant \epsilon_1 \\ 0 & \text{otherwise} \end{cases} \tag{15}$$

then it can be shown that as $u \to 0$ that

$$\psi^*(u) \sim 1 - u\bar{t} + O(u^2) \qquad \text{if} \quad T > T_0 \tag{16}$$

and

$$\psi^*(u) \sim 1 - (\text{const})u^{T/T_0} \qquad \text{if} \quad T < T_0 \tag{17}$$

Equation (16) will lead, for large t, to

$$\langle l_x(t)\rangle \sim \frac{\bar{l}_x}{\bar{t}}\, t \tag{18}$$

while Eq. (17) yields

$$\langle l_x(t)\rangle \sim \bar{l} t^{\beta} \tag{19}$$

where

$$\beta = T/T_0 \tag{20}$$

Note that the velocity of the dislocation becomes in Eq. (19)

$$\frac{d\langle l_x(t)\rangle}{dt} \sim \frac{T}{T_0} \bar{l} t^{\beta-1} \tag{21}$$

Thus there is more resistance to transport at lower temperatures. Such behavior has been seen in experiments on the penetration of rigid projectiles into epoxy resins.[10]

4. COMPARISON WITH EXPERIMENT

As seen in Fig. 1 there is an early stage for imparting momentum into the target which is followed by a late stage where axial and radial momentum obey the same scaling. Initially, we assume $T > T_0$ in the early stage, and when T settles down to a value below T_0 there is a crossover to the late stage flow. This is characterized by the difference between Eqs. (18) and (19). Here we will only discuss the late stage flow. The momentum

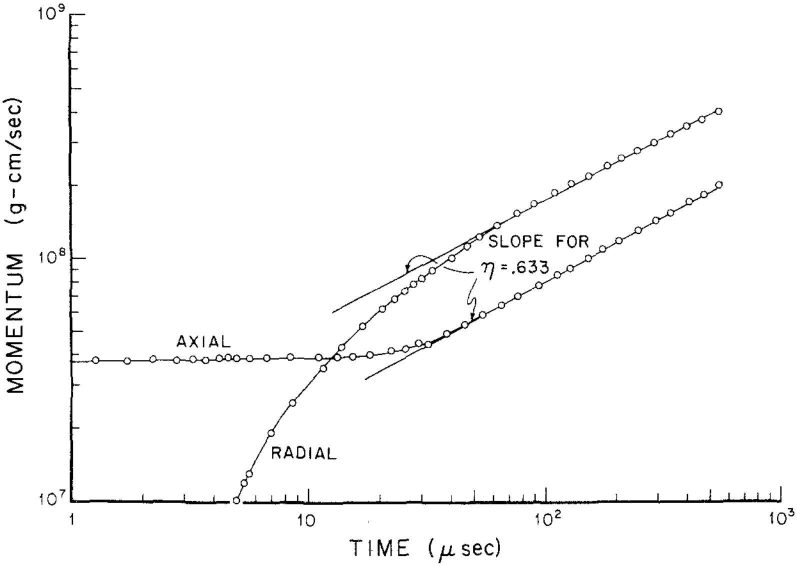

Fig. 1. Radial and axial momenta redrawn from Ref. 3. The experimental slopes have $\beta = \alpha/(1 + \alpha) = 0.367$, $\alpha = 0.59$, $\eta = 1 - \beta$.

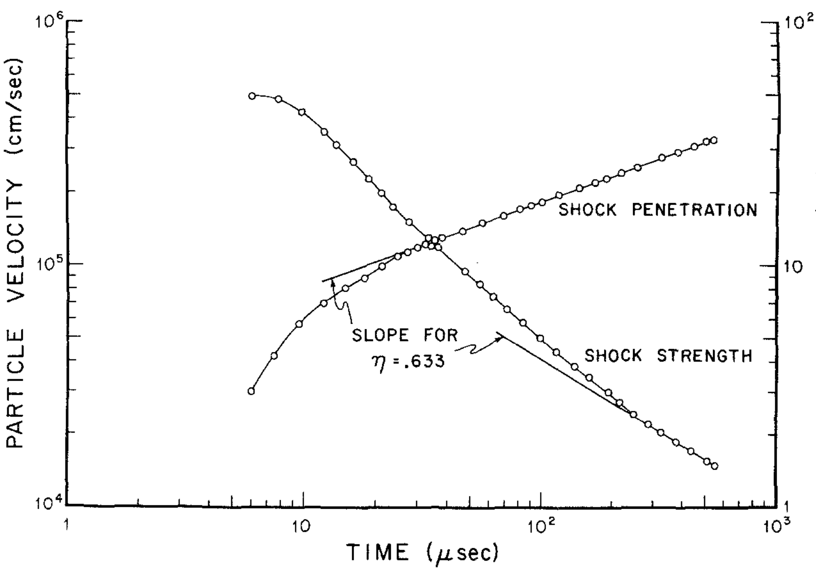

Fig. 2. Shock penetration and shock strength versus time, redrawn from Ref. 3.

$I(t)$ transferred to the target involves the mass engulfed which grows as $\langle l_x(t)\rangle^3 \sim t^{3\beta}$ (since the initial x-direction bias now changes to an outward radial bias) and the velocity which scales as $t^{\beta-1}$. Thus

$$I(t) \sim t^{4\beta-1} \tag{22}$$

In Fig. 1 I scales as $t^{0.468}$ at late times indicating that $\beta = 0.367$ or in terms of temperature that $T = 0.367 T_0$ is the condition for the onset of the late stage flow. We now see that the conservation law $Mv_0^{3\alpha} = \text{const}$ arises from the scaling

$$(Lv_0^{\alpha})^3 = \text{const} \tag{23}$$

where L^3 is proportional to the mass of the projectile, or

$$l \sim t^{\alpha/(1+\alpha)} \tag{24}$$

where l^3 is proportional to the mass engulfed by the spreading deformation.

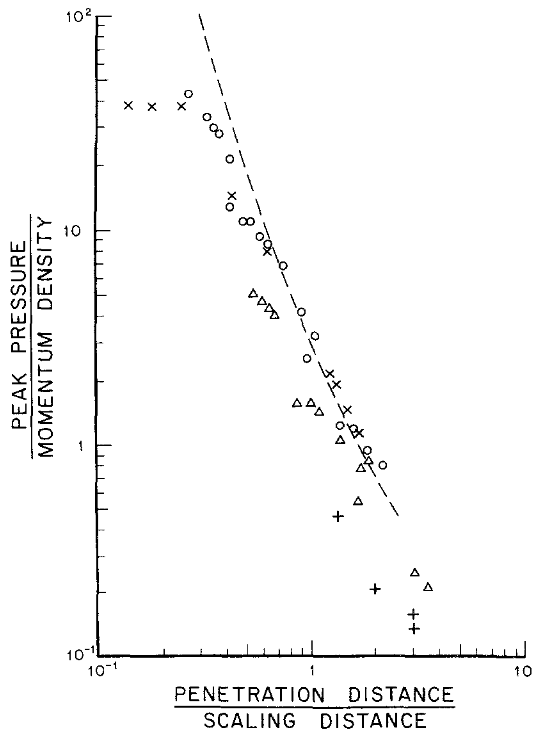

Fig. 3. Peak pressure on the symmetry axis, compared with approximate point-source-similitude prediction, redrawn from Ref. 11 in which the individual experiments are referenced.

We set $\beta = \alpha(1 + \alpha)^{-1}$ to match Eqs. (19) and (24). An α of 0.59 corresponds to a β of 0.367.

We can also express the deformation velocity in terms of $\langle l_x(t)\rangle$ using Eqs. (19) and (21), as

$$\frac{d}{dt}\langle l_x(t)\rangle \sim \langle l_x(t)\rangle^{(\beta-1)/\beta} = \langle l_x(t)\rangle^{-1/\alpha} \tag{25}$$

We interpret Eq. (25) as the way the velocity of the shock decreases with penetration distance into the target. The pressure $P(t)$ has units of energy/volume, so we can write

$$P(t) \sim \left[\frac{d}{dt}\langle l_x(t)\rangle\right]^2 \sim \langle l_x(t)\rangle^{-2/\alpha} \tag{26}$$

as the pressure associated with the deformation of the metal with the passage of the shock wave. Pressure measurements from a number of different experiments are shown in Fig. 3 and agree with Eq. (26) with an $\alpha = 0.58$.[11] In Fig. 2 the penetration of the shock as well as its strength is shown as a function of time. The late stage behavior can be understood in terms of our model. The early time behavior and crossover regime are not as well understood.

REFERENCES

1. H. Scher and E. W. Montroll, *Phys. Rev. B* **12**:2455 (1975).
2. G. Pfister and H. Scher, *Adv. Phys.* **27**:747 (1978).
3. J. K. Dienes and J. M. Walsh in *High Velocity Impact Phenomena*, R. Kinslow, ed. (Academic Press, New York, 1979).
4. A. S. Krausz and H. Eyring, *Deformation Kinetics* (Wiley-Interscience, New York, 1975).
5. E. W. Montroll and G. H. Weiss, *J. Math. Phys.* **6**:178 (1965).
6. M. F. Shlesinger, *J. Stat. Phys.* **10**:421 (1974).
7. J. Klafter and R. Silbey, *Phys. Rev. Lett.* **44**:55 (1980).
8. V. M. Kenkre, E. W. Montroll, and M. F. Shlesinger, *J. Stat. Phys.* **9**:45 (1973).
9. W. Feller, *An Introduction to Probability Theory and Its Application*, Vol. 2 (Wiley, New York, 1966), pp. 186, 360.
10. T. Shioya and K. Kawata, in *High Velocity Deformation of Solids*, IUTAM Sym. K. Kawata and T. Shioiri, eds. (Springer-Verlag, Berlin, 1978).
11. W. J. Rae in *High Velocity Impact Phenomena*, R. Kinslow, ed. (Academic Press, New York, 1979) p. 277.